*Journal of Applied Fluid Mechanics*, Vol. 10, No. 6, pp. 1773-1783, 2017.
Available online at www.jafmonline.net, ISSN 1735-3572, EISSN 1735-3645.
DOI: 10.29252/jafm.73.245.27892

# A Balloon Model Examination with Impulsion of Cu-Nanoparticles as Drug Agent through Stenosed Tapered Elastic Artery

S. Ijaz[1†] and S. Nadeem[2]

[1]*Department of Mathematics, Faculty of Sciences, HITEC University, Taxila, Pakistan.*
[2]*Department of Mathematics, Quaid-i-Azam University, Islamabad, Pakistan*

†*Corresponding Author Email: shaguftaijaz88@gmail.com*

(Received April 21, 2017; accepted June 7, 2017)

## ABSTRACT

In this speculative examination, main focused is to address Cu-nanoparticles application in an inclined stenosed elastic artery with balloon model examination. Flow of blood in an inclined stenotic artery is investigated mathematically by considering its behavior as viscous fluid. The dimensionless terms of temperature, velocity, resistance to blood flow and stress on wall of stenotic inclined artery has been computed by using mild stenosis approximation. The model is also used to understand the significance of overlapping stenosed artery with tapered angle and inclination angle. At the end, the results confirmed that the impulsion of copper as drug agent minimized the amplitude of the resistance to blood flow and hence nanoparticles plays an important role in engineering as well in biomedical applications.

**Keywords**: Blood flow; Overlapping stenosis; Balloon model; Cu-Nanoparticles.

## NOMENCLATURE

| | | | |
|---|---|---|---|
| $e_o$ | normal artery radius | $u_o$ | averaged velocity |
| $F$ | rate of flow | | |
| $G_r$ | Grashof number | $\omega$ | angular frequency |
| $h(z)$ | stenosis height | $\rho$ | density |
| $k$ | thermal conductivity | $(\rho c_p)$ | heat capacitance |
| $L$ | artery length | $\delta$ | height of stenosis |
| $L_O$ | length of stenosis | $\beta$ | heat source parameter |
| $p$ | pressure force | $\Phi$ | nanoparticle volume fraction |
| $R_{en}$ | Reynolds number | $\theta$ | nano dimensionless temperature |
| $r, z$ | radial and axial directions | $d^*$ | position of stenosis |
| $S_{rz}$ | stress on wall | $\lambda$ | resistance to blood |
| t | time | $\varphi$ | shape parameter |
| $T_o$, $T_1$ | temperature considered on walls | $\gamma$ | thermal expansion |

## 1. INTRODUCTION

Atherosclerosis is a syndrome of arteries which involve complex interactions between blood flow and the artery wall. Hemodynamics factors, such as resistance impedance to flow and wall shear stress plays very important role in keeping normal vascular endothelial function which is directly associated to the generation and propagation of the atherosclerotic lesion. The higher resistance to flow can also become progressively important as the stenosis becomes more severe. The development of stenosis causes to block circulation of blood in the heart which may result numerous cardiovascular diseases such as angina, myocardial infarction etc. The actual reason for growth of stenosis in an artery is not known, but its impact on the flow features has been considered by many researchers i.e., Texon (1957), Young *et al*. (1973), Liu and Tang (2000), Mandal *et al*. (2011), Nadeem and Ijaz (2016).

Several investigates about stenotic growth indicate that the studies are mostly concerned with the particular stenosis while the stenosis may progress in the sequence or may be of asymmetrical shapes or of composite or overlapping in nature. Chakravarty *et al*. (1996) explored mathematical problem related to blood flow through tapered wall segments. They considered non-linear and two-dimensional blood flow mathematical model in stenotic arteries with the accumulation of overlapped stenosis. Mekheimer *et al*. (2008) explored theoretical model of an elastic stenosed artery. They discussed here the impact of induced magnetic field on flow of blood. Ismail *et al*. (2008) explored non-newtonian model of blood with an elastic stenosed artery. Mekheimer *et al*. (2012) deliberated the behavior of blood flow through anisotropically tapered stenosed artery in presence of heat and chemical reactions. They treated here nature of blood in arteries as non-newtonian micropolar fluid.

In recent study of medicine, with the advancement of coronary balloon angioplasty, there has been a significant increase in the use of catheters of several sizes to minimize the stenotic effects. The insertion of a catheter in a blood vessel will change the flow field. Dash *et al*. (1996) explored pattern of blood in stenotic arteries. They found here that resistance increases due to catheterization. Mekheimer *et al*. (2010) explored the analysis of a dusty model for the axis-symmetric flow of blood through coaxial tubes. Verma *et al*. (2011) deliberated mathematical problem of artery catheterization by assuming symmetric stenosis with blood flow model. For further analysis see references Sankar and Hemalatha (2007), Srivastava and Srivastava (2009), Mekheimer *et al*. (2012).

Theoretical models with arteries carrying blood that are cited above were considered to being horizontal however it is well known that in numerous investigation all vessels in physiological systems are not horizontal because some have inclination to the axis. Chakraborty *et al*. (2011) explored the mathematical model of an inclined artery by considering radially symmetric stenosis. They discussed the slip at stenotic wall, hematocrit and inclination of the artery. Mekheimer *et al*. (2015) examined the theoretical analysis of inclined catheterized arteries with balloon angioplasty. To discuss this analysis, here they considered blood in arteries as Carreau fluid. For some further important studies in this direction are given in Prasad *et al*. (2008), Mohan *et al*. (2013).

In engineering and medical sciences nanofluid keeps several unique features. Nanofluid enhances thermal conductivity of the considered base fluid immensely, which are stable and have no further problems such as erosion and sedimentation. Recent, study has revealed that they are important for improving the heat transport and thermal conductivity properties of the base fluid and may have potential applications in the field of biomedicine. In fact, Choi (1995) was the first who presented the experimental measurements and thermal conductivity enhancement for the thermal conductivity of nanofluids. Later on some other investigators explored different mathematical nano models cited as Buongiorno (2005), Nadeem and Ijaz (2015). Ellahi *et al*. (2014) explored the non-newtonian mathematical model of nanofluid with tapered stenotic artery. Nadeem and Ijaz (2015) explored nanoparticles examination through stenotic artery with permeable walls. They deliberated here solid nanoparticles consequence of a curved stenotic artery. Nadeem and Ijaz (2016) explored the nanoparticles possessions by considering mathematical nano blood flow models. They concluded that impact of hemodynamics of a stenotic artery minimizes by introducing nanoparticles. Some more useful analysis is given in the references Jiang *et al*. (2007), Gentile *et al*. (2007), Akbarzadeh *et al*. (2016).

With the above theoretical inspirations, an inclined vessel with overlapped stenotic region is considered in this examination. The catheterization effect with help of balloon model is also assumed. The dimensional governing equations are simplified after using mild stenosis approximation. After this approximation differential equation are solved by using exact technique. The acquired effects of hemodynamics have been deliberated for various parameters with the help of graphical illustration. At the end of this investigation, we note that use of nanoparticles as drug agent minimizes the hemodynamics of stenotic artery.

## 2. FORMULATION OF THE PROBLEM

To proceed this analysis, unsteady, incompressible and viscous nanofluid is considered that flows through a stenotic artery of finite length L. Also to discuss the nano effects heat transfer existence is introduced by considering temperature $T_0$ at the inner wall of balloon and temperature $T_1$ at the wall of stenotic artery. The configuration of stenotic segment is defined as [6]

$$\bar{h}(z,t) = [(a^*z + e_0) - \frac{\delta^* \cos\phi}{L_0}(\bar{z} - e^*)\{11 - \frac{94}{3L_0}(\bar{z} - e^*) + \frac{32}{L_0^2}(\bar{z} - e^*)^2 - \frac{32}{3L_0^2}(\bar{z} - e^*)^3\}]$$

$$x_1(t), \qquad e^* \le \bar{z} \le e^* + \frac{3}{2L_0}$$

$$= (a^*\bar{z} + e_0)x_1(t) \qquad \text{otherwise}, \tag{1}$$

in above $\bar{h}(z,t)$ is the stenotic radius, $e_0$ is the non-stenotic radius, $\phi$ is the tapered angle, $\delta\cos\varphi$ is critical height of the stenotic segment, $\frac{3}{2L_0}$ is the length, $e^*$ is position and $a^* = \tan\varphi$ is the slope of the stenotic vessel. Different possible shapes of artery are analyzed by considering $\varphi < 0$ for convergent shape, $\phi = 0$ for non-tapered shape and $\varphi > 0$ for divergent shape. The time-variant parameter is defined as

$$x1(t) = 1 - c(\cos wt - 1)\exp[-cwt], \tag{2}$$

where $c$ is defined as constant, $w$ as the angular frequency and $t$ as time. Balloon model is defined as

$$\begin{aligned}\overline{H}(z) &= e_0\{k + \delta_1 \exp[-\pi^2(z - z_d - \\ &\quad 0.5)^2]\}, \ e^* \le \bar{z} \le e^* + \frac{3}{2L_0}, \\ &= e_0 k \qquad \text{otherwise},\end{aligned} \tag{3}$$

where $\delta_1$ is the maximum height of balloon and is attained at $z = z_d + 0.5$, $e_0 k$ is the radius of the balloon, $z_d$ is the axial translation of the balloon.

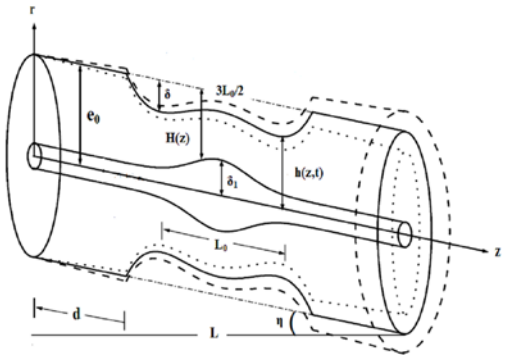


**Fig. 1. Configuration of overlapped stenotic artery.**

The formulated equations in the presence of nanoparticles can be written as,

$$\frac{\partial \bar{v}}{\partial \bar{r}} + \frac{\bar{v}}{\bar{r}} + \frac{\partial \bar{w}}{\partial \bar{z}} = 0, \tag{4}$$

$$\rho_{nf}\left(\frac{\partial \bar{v}}{\partial \bar{t}} + \bar{v}\frac{\partial \bar{v}}{\partial \bar{r}} + \bar{w}\frac{\partial \bar{v}}{\partial \bar{z}}\right) = -\frac{\partial \bar{p}}{\partial \bar{r}} + \mu_{nf}\left(\frac{\partial^2 \bar{v}}{\partial \bar{r}^2} + \frac{1}{\bar{r}}\frac{\partial \bar{v}}{\partial \bar{r}} + \frac{\partial^2 \bar{v}}{\partial \bar{z}^2} - \frac{\bar{v}}{\bar{r}^2}\right) - g(\rho\gamma)_{nf}(\bar{T} - \bar{T}_1)\cos\eta, \tag{5}$$

$$\rho_{nf}\left(\frac{\partial \bar{w}}{\partial \bar{t}} + \bar{v}\frac{\partial \bar{w}}{\partial \bar{r}} + \bar{w}\frac{\partial \bar{w}}{\partial \bar{z}}\right) = -\frac{\partial \bar{p}}{\partial \bar{z}} + \mu_{nf}\left(\frac{\partial^2 \bar{w}}{\partial \bar{r}^2} + \frac{1}{\bar{r}}\frac{\partial \bar{w}}{\partial \bar{r}} + \frac{\partial^2 \bar{w}}{\partial \bar{z}^2}\right) + g(\rho\gamma)_{nf}(\bar{T} - \bar{T}_1)\sin\eta, \tag{6}$$

$$\left(\frac{\partial \bar{T}}{\partial \bar{t}} + \bar{v}\frac{\partial \bar{T}}{\partial \bar{r}} + \bar{w}\frac{\partial \bar{T}}{\partial \bar{z}}\right) = \frac{k_{nf}}{(\rho c_p)_{nf}}\left(\frac{\partial^2 \bar{T}}{\partial \bar{r}^2} + \frac{1}{\bar{r}}\frac{\partial \bar{T}}{\partial \bar{r}} + \frac{\partial^2 \bar{T}}{\partial \bar{z}^2}\right) + \frac{q_0}{(\rho c_p)_{nf}}, \tag{7}$$

in above equation $\bar{v}$ and $\bar{w}$ is the velocity components, $\bar{T}$ is the temperature, $q_0$ is the heat generation parameter. For the considered single nano phase model $k_{nf}$ denotes thermal conductivity, $\mu_{nf}$ is the viscosity, $\rho_{nf}$ is the density, $(\rho c_p)_{nf}$ is the heat capacitance, $\gamma_{nf}$ is the thermal expansion coefficient and the thermo physical properties are given as (see Table (1))

**Table 1 Thermophysical properties of base fluid and solid nanoparticles**

| Properties | Blood | Cu |
|---|---|---|
| $c_p$ | 3594 | 385 |
| $\rho$ | 1063 | 8933 |
| $k$ | 0.492 | 400 |
| $\gamma$ | 0.18 | 1.67 |

$$\begin{aligned}\frac{\mu_{nf}}{\mu_f} &= \frac{1}{(1-\Phi)^{2.5}}, \ \alpha_{nf} = \frac{k_{nf}}{(\rho c_p)_{nf}}, \\ \frac{\rho_{nf}}{\rho_f} &= (1-\Phi) + \Phi\frac{\rho_s}{\rho_f}, \\ \frac{(\rho c_p)_{nf}}{(\rho c_p)_f} &= (1-\Phi) + \frac{(\rho c_p)_s}{(\rho c_p)_f}\Phi, \\ \frac{(\rho\gamma)_{nf}}{(\rho\gamma)_f} &= (1-\Phi) + \frac{(\rho\gamma)_s}{(\rho\gamma)_f}\Phi, \\ k_{nf} &= k_f\left[\frac{(k_s + 2k_f) - 2\Phi(k_f - k_s)}{(k_s + 2k_f) + \Phi(k_f - k_s)}\right],\end{aligned} \tag{8}$$

where $\rho_f$ denotes the density, $\mu_f$ is the viscosity, $\gamma_f$ is thermal expansion coefficient, $(\rho c_p)_f$ is the heat capacitance and $k_f$ is thermal conductivity of considered base fluid, while $\rho_s$ denotes the density, $\gamma_s$ is the thermal expansion coefficient, $(\rho c_p)_s$ is the heat capacitance, $\Phi$ is the nanoparticle volume fraction and $k_s$ is the thermal conductivity of the considered solid nanoparticles. Non dimensional parameters are defined as,

$$\begin{aligned}r &= \frac{\bar{r}}{e_0}, \ z = \frac{\bar{z}}{L_0}, \ w = \frac{\bar{w}}{u_o}, \ v = \frac{L_0\bar{v}}{u_o\delta}, \\ p &= \frac{e_0^2\bar{p}}{u_o L_0 \mu_f}, \ t = \frac{\bar{t}u_o}{L_0}, \ R_{en} = \frac{e_0 u_o \rho_f}{\mu_f}, \\ G_r &= \frac{g\gamma_f\rho_f e_0^2(T_0 - T_1)}{u_0\mu_f}, \ \beta = \frac{q_0 e_0^2}{(T_0 - T_1)k_f}, \\ \theta &= \frac{T - T_1}{T_0 - T_1}.\end{aligned} \tag{9}$$

Where in above equation $R_{en}$ denotes the Reynolds

number, $G_r$ is the Grashof number, $\beta$ is the heat source parameter and $u_0$ is the averaged velocity. By mean of Eq. (9) and considered approximations (mild stenosis $\delta^* = \frac{\delta}{e_0} \prec\prec 1$ and $\varepsilon = \frac{e_0}{b} \approx O(1)$), the formulated Eqs. (5) to (7) can be reduced as

$$\frac{\partial p}{\partial r} = 0, \tag{10}$$

$$\frac{\partial p}{\partial z}(1-\Phi)^{2.5} =$$

$$\frac{\partial^2 w}{\partial r^2} + \frac{1}{r}\frac{\partial w}{\partial r} + (1-\Phi)^{2.5}\frac{(\rho\gamma)nf}{(\rho\gamma)f}\sigma 4\theta, \tag{11}$$

$$\frac{\partial^2 \theta}{\partial r^2} + \frac{1}{r}\frac{\partial \theta}{\partial r} + \beta\sigma 2\sigma 3 = 0, \tag{12}$$

where

$$\begin{aligned} &\sigma_1 = (1-\Phi) + \Phi\frac{(\rho c_p)_s}{(\rho c_p)_f},\ \sigma_2 = \frac{1}{\sigma_1}, \\ &\sigma_3 = \sigma_1\left(\frac{(1-\Phi)k_s + (\Phi+2)k_f}{(2\Phi+1)k_s + 2(1-\Phi)k_f}\right) \\ &\sigma_4 = \left((1-\Phi) + \Phi\frac{\rho_s\gamma_s}{\rho_f\gamma_f}\right)(1-\Phi)^{2.5}G_r\sin\eta. \end{aligned} \tag{13}$$

The geometry of arterial stenosis and balloon model in dimensionless form are defined as

$$\begin{aligned} h(z,t) = [(az+1) - \delta\cos\phi(z-\sigma^*)\{11 - \frac{94}{3} \\ (z-\sigma^*) + 32(z-\sigma^*)^2 - \frac{32}{3}(z-\sigma^*)^3\}] \\ x_1(t), \qquad \sigma^* \le z \le \sigma^* + \frac{3}{2} \\ = (az+1)x_1(t) \qquad \text{otherwise}, \end{aligned} \tag{14}$$

with

$$\delta = \frac{\delta^*}{e_0},\ \sigma^* = \frac{e^*}{L_0},\ a^* = \frac{aL_0}{e_0}. \tag{15}$$

And

$$\begin{aligned} H(z) = k + \delta_1\exp[-\pi^2 L_0^2(z - \\ \frac{(z_d+0.5)}{L_0})^2],\ \sigma^* \le z \le \sigma^* + \frac{3}{2}, \\ = k \qquad \text{otherwise}. \end{aligned} \tag{16}$$

Corresponding boundary conditions are defined as

$$w = 0 \ \ at \ \ r = h(z,t),\ \ w = 0 \ \ at \ \ r = h(z,t), \tag{17}$$

$$\theta = 0 \ \ at \ \ r = h(z,t),\ \ \theta = 1 \ \ at \ \ r = H(z). \tag{18}$$

The exact solutions of Eqs. (11) and (12) using Eqs. (17) and (18) are directly written as

$$\begin{aligned} \theta = \frac{1}{4(\ln(h)-\ln(H))}(4(\ln(h)-\ln(H)) + \beta\sigma_2\sigma_3 \\ (h^2(\ln(r)-\ln(H)) + r^2(-\ln(h)+\ln(H)) + \\ (\ln(h)-\ln(r))H^2)), \end{aligned} \tag{19}$$

$$\begin{aligned} w = \frac{dp}{dz}\frac{(1-\Phi)^{2.5}}{4(\ln(h)-\ln(H))}((H^2-r^2)\ln(h) + (-h^2 + \\ r^2)\ln(H) + (h^2-H^2)\ln(r)) + \frac{1}{64(\ln(h)-\ln(H))^2} \\ (-16((-H^2+r^2)(\ln(h))^2 + (-h^2+H^2)\ln(r) + \\ (H^2-r^2)\ln(h)(-1+\ln(h)+\ln(r)) + \ln(h)(h^2 - \\ r^2 + (-H^2+r^2)\ln(r))) + \beta((3H^4 - 4H^2r^2 + r^4) \\ (\ln(h))^2 + (3h^4 - 4h^2r^2 + r^4)(\ln(H))^2 - 4 \\ (h^2-H^2)^2\ln(r) - (h^2-H^2)\ln(H)(-4h^2 + 4r^2 + \\ (3(h^2+H^2) - 4r^2)\ln(r)) + \ln(h)((-3(h^4+H^4) + \\ 4(h^2+H^2)r^2 - 2r^4)\ln(H) + (h^2-H^2)(-4H^2 + \\ 4r^2 + (3(h^2+H^2) - 4r^2)\ln(r)))\sigma_2\sigma_3)\sigma_4). \end{aligned} \tag{20}$$

Expression of flow rate is defined as

$$F = \int_H^h rw dr. \tag{21}$$

Using Eq. (20) into Eq. (21), expression of pressure gradient is given as

$$\frac{dp}{dz} = -\frac{F - A(z)}{\frac{(1-\Phi)^{2.5}}{16}\left(h^4 - H^4 + \frac{(h^2-H^2)^2}{-\ln(h)+\ln(H)}\right)}, \tag{22}$$

where

$$\begin{aligned} A(z) = \frac{1}{384(\ln(h)-\ln(H))^2}(6(-4(h^2-H^2)^2 + \\ (\ln(h)-\ln(H))(3h^4 + 4h^2H^2 - 7H^4 + 4H^4 \\ (-\ln(h)+\ln(H)))) + \beta(h^2-H^2)(6 \\ (h^2-H^2)^2 + (-9h^4 + 9H^4 + 4(h^4 + h^2H^2 + \\ H^4)(\ln(h)-\ln(H)))(\ln(h)-\ln(H)))\sigma_2\sigma_3)\sigma_4. \end{aligned} \tag{23}$$

Pressure drop through overlapped stenotic artery is given as

$$\Delta p = \int_0^L\left(-\frac{dp}{dz}\right)dz. \tag{24}$$

Using Eq. (24), the resistance to blood can be estimated as

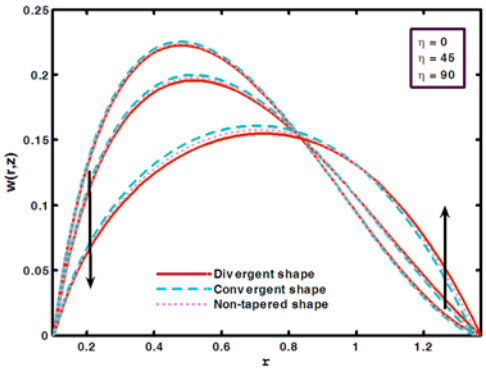


**Fig. 2. Velocity profile for $\Phi=0.01$.**

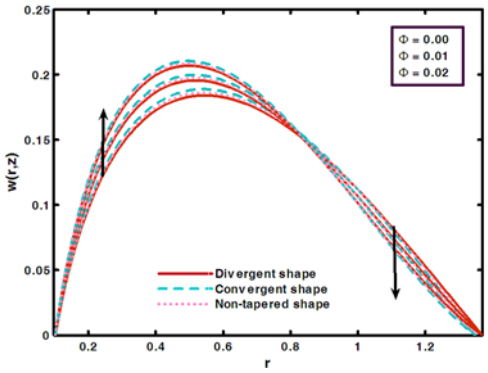


**Fig. 3. Velocity profile for $\eta=45$.**

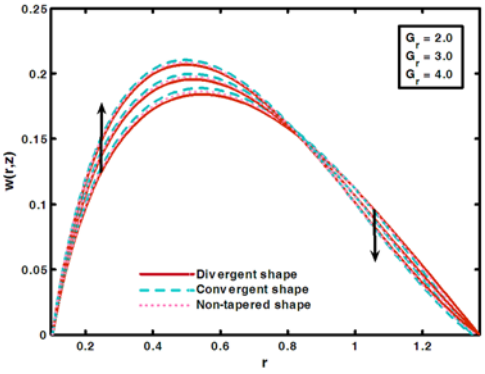


**Fig. 4. Velocity profile for $\beta=2.0$.**

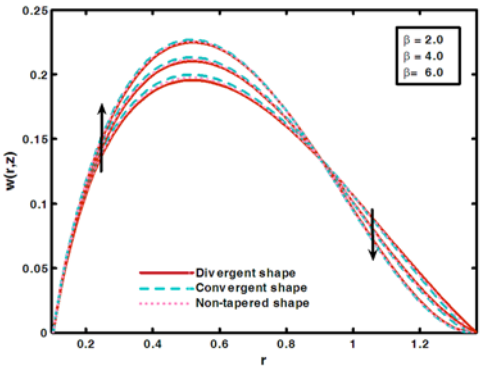


**Fig. 5. Velocity profile for $G_r=2.0$.**

$$\lambda=\frac{\Delta p}{F}=\int_{0}^{\sigma^*} M(z)|_{h=(az+1)x_1(t)}\,dz+\int_{\sigma^*}^{\sigma^*+\frac{3}{2}} N(z)dz+\int_{\sigma^*+\frac{3}{2}}^{L} M(z)_{h=(az+1)x_1(t)}dz, \tag{25}$$

where

$$M(z)=N(z)|h=(az+1)x_1(t),\ H=k\ . \tag{26}$$

To evaluate the stresses on the wall of artery following expression is considered [6]

$$S_{rz}=-\frac{\mu_{\eta f}}{\mu f}\left(\frac{\partial w}{\partial r}\right)_{r=h}. \tag{27}$$

Above Eqs. (27) and (25) are further solved by using Mathematica software

## 3. GRAPHICAL RESULTS AND DISCUSSION

In this unit for theoretical examination figures of wall shear stress, resistance, velocity, temperature profile and streamlines are plotted with the help of physical parameters such as the Grashof number $G_r$, heat source parameter $\beta$, inclination angle $\eta$ and nanoparticles volume fraction $\Phi$ . These parameters are kept constant such as $\eta=45$, $\delta=0.01$, $\sigma^*=0.75$, $F=0.1$, $t=0.5$, $G_r=2.0$, $\omega=7.854$, $\beta=2.0$ , $\delta_1=0.01$, $z_d=0.1$, $k=0.1$, $\Phi$=0.01. The graphs of axial velocity $w$ against $r$ for overlapping stenosis are given in Figs. (2) to (5). The variation of inclination angle $\eta$ is given in Fig. (2). It is observed from this graph that velocity starts decreasing near the wall of the balloon between the interval $H\le r\le 1.0$ (at $\eta=90$) , $H\le r\le 0.85$ (at $\eta$=0 and $\eta$=45) and higher magnitude for convergent shape is depicted in these regions, while opposite behavior is depicted near wall of stenotic artery in the region $1.01\le r\le h$ (at $\eta$=90) , $0.86\le r\le h$ (at $\eta$=0 and $\eta=45$) . Figs. (3) to (5) shows the variations for Grashof number $G_r$ , heat source parameter $\beta$ and nanoparticles volume fraction $\Phi$ on the graphs of velocity profile. It is depicted that velocity profile gives higher magnitude for convergent shape and start increasing near balloon wall of in the region $H\le r\le 0.86$, while opposite behavior is depicted near arterial wall in the region $0.87\le r\le h$. The phenomenon of nano temperature profile is given in Figs. (6) and (7). It is depicted that the nano temperature profile increases with an increase in the values of heat source parameter $\beta$. This result is obtained due to increase in the thermal behavior of

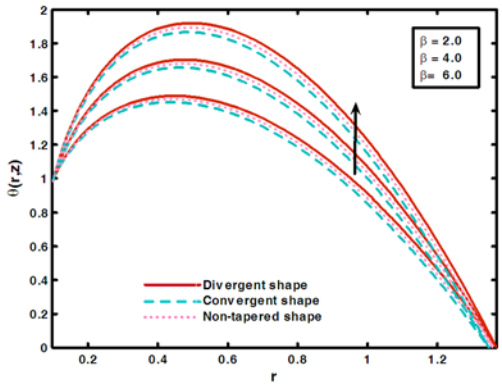


**Fig. 6. Nano temperature distribution for $\Phi=0.01$.**

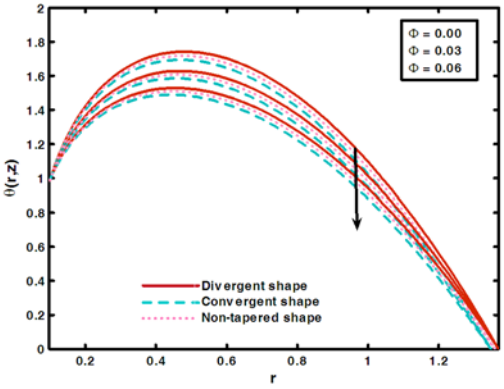


**Fig. 7. Nano temperature distribution for $\beta=2.0$.**

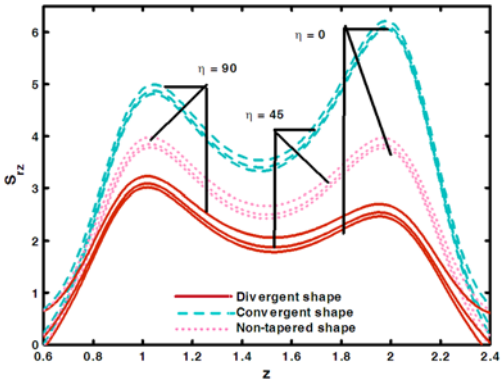


**Fig. 8. Stress on wall for $\Phi=0.01$.**

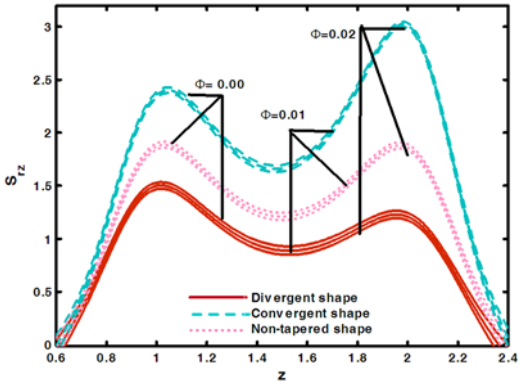


**Fig. 9. Stress on wall for $\eta=45$.**

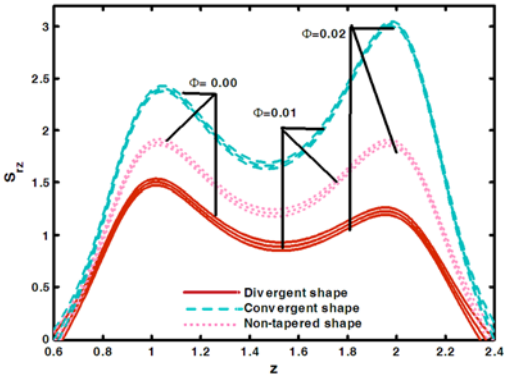


**Fig. 10. Stress on wall for $\beta=2.0$.**

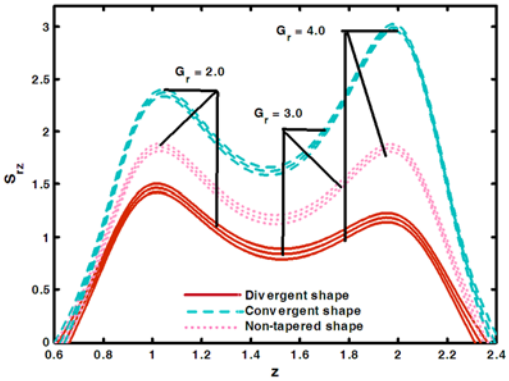


**Fig. 11. Stress on wall for $G_r=2.0$.**

the base fluid, while decreases with an increase in the nanoparticle volume fraction. The graph of the temperature phenomena gives higher magnitude for divergent shape when compare to other shapes. Figs. (8) to (11) are plotted to understand stress behavior on wall of stenotic artery. From these graphical illustrations one may analyze that stresses on the wall of inclined stenotic artery start decreasing towards the downstream of the stenotic region and then start rapidly increasing towards the end of the inclined stenotic artery. One may also analyze from these stress patterns that convergent shape of an artery gives higher magnitude when compared to other non-tapered and divergent shapes of stenotic artery. The stresses behavior for parameters inclination angle $\eta$ and nanoparticles volume fraction $\Phi$ are given in Figs. (8) and (9). It is depicted under this stress pattern that with an increase in the inclination angle $\eta$ stresses on wall of an inclined stenotic artery decreases, while stresses on wall decreases by increasing in the concentration of nanoparticles. Figs. (10) and (11) relates the stress with different parameters such as Grashof number $G_r$ and heat

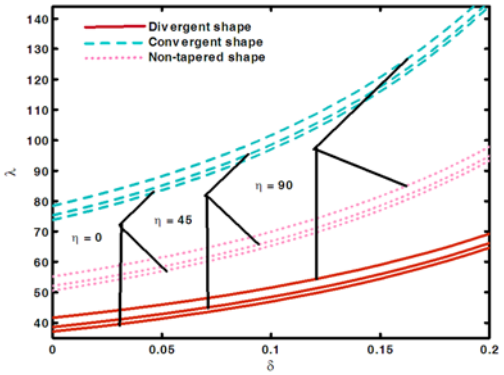


**Fig. 12. Resistance to blood for $\Phi=0.01$.**

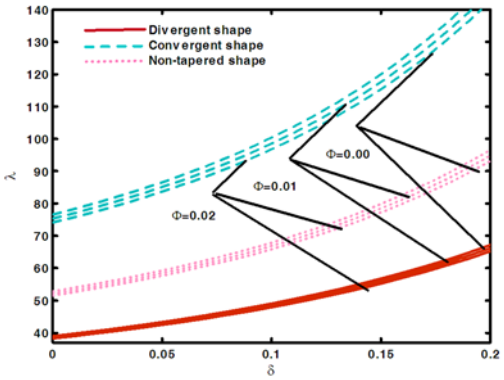


**Fig. 13. Resistance to blood for $\eta=45$.**

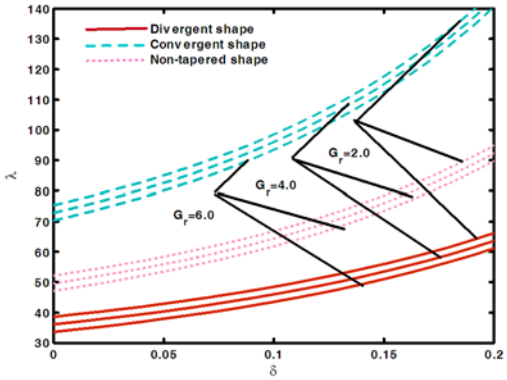


**Fig. 14. Resistance to blood for $\beta=0.2$.**

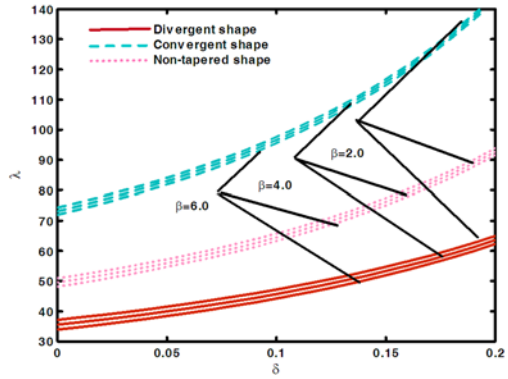


**Fig. 15. Resistance to blood for $G_r=2.0$.**

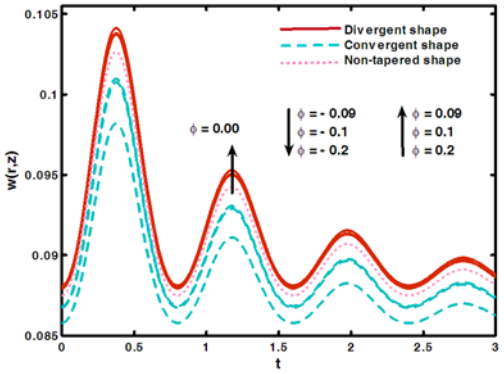


**Fig. 16. Chart of velocity profile with $t$.**

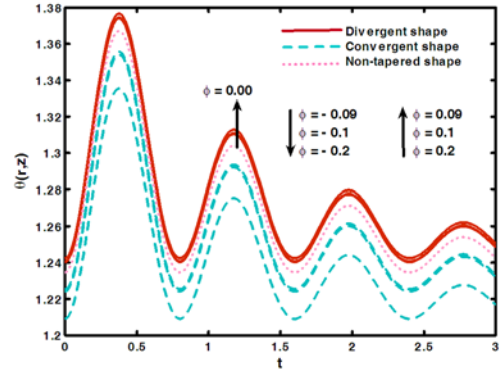


**Fig. 17. Chart of temperature profile with $t$.**

source $\beta$. It is depicted from this pattern that the stresses on wall of stenotic inclined artery decreases with an increase in Grashof number $G_r$ and heat source $\beta$. Figs. (12) to (15) are strategized to show the variation of resistance to flow versus the height of stenosis $\delta$with different shape of inclined artery. It is observed that resistance to flow gives higher magnitude for convergent shape as comparing to other shapes and increases with an increase in the height of stenosis. The graphical illustration for inclination angle $\eta$and nanoparticles volume fraction $\Phi$ is given in Figs. (12) and (13). It is analyzed from this pattern that resistance to flow increases with an increase in inclination angle $\eta$, while opposite behavior is depicted for nanoparticles volume fraction case. Fig. (14) is plotted for Grashof number $G_r$ and noted that resistance to flow reduces with an increase in $G_r$ . The inspiration of heat source parameter $\beta$ on resistance to flow is plotted in Fig. (15). One may depict from this figure that resistance to flow minimizes with an increase in $\beta$. Figs. (16) to (19) represent the behavior of wall shear stress and resistance to blood flow against time $t$ for almost three cyclic phases. One regular observation from

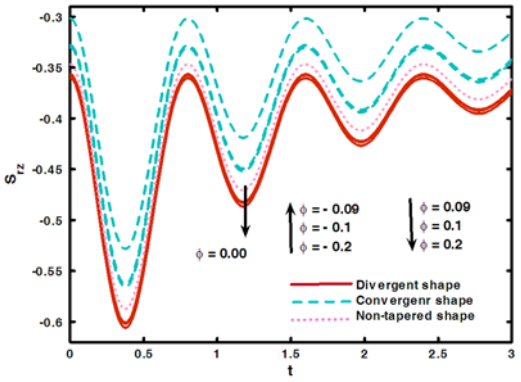


**Fig. 18. Chart of stress on wall with $t$**

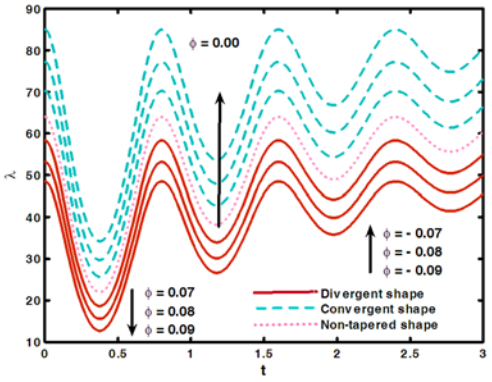


**Fig. 19. Chart of resistance to blood with $t$**

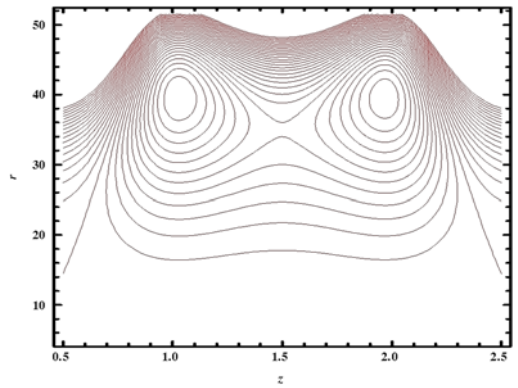


**Fig. 20. Blood flow configuration for $G_r = 2.8$.**

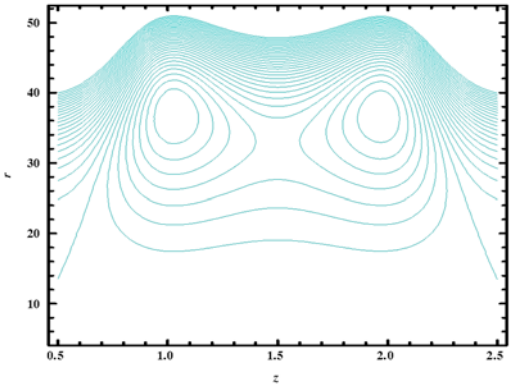


**Fig. 21. Blood flow configuration for $G_r = 3.2$.**

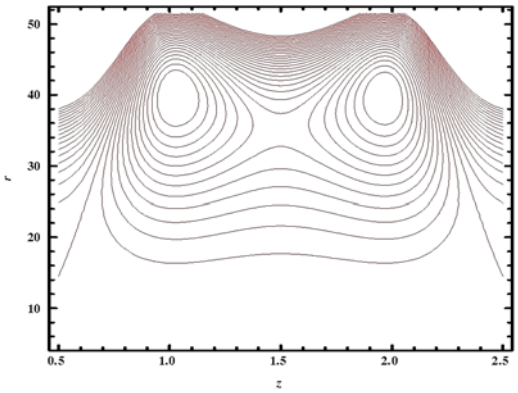


**Fig. 22. Blood flow configuration for $\beta = 0.46$.**

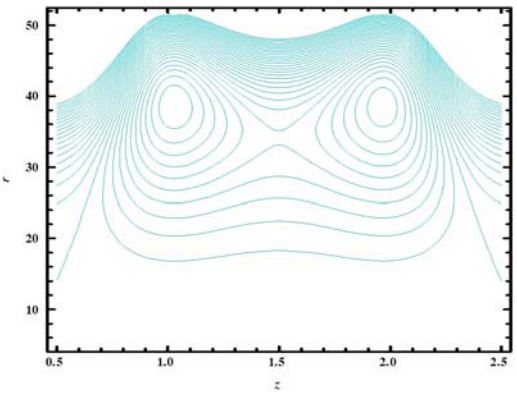


**Fig. 23. Blood flow configuration $\beta = 0.50$.**

these figures is that the magnitude of first cycle starts with decreasing behavior to obtain its least possible value and after this it starts increasing towards its extreme value. This similar pattern is observed for other remaining cycles. It is also analyzed that oscillated cycles decay as time $t$ increases. This graphical result also shows that the stresses on the wall and resistance to blood flow decreases for converged stenotic inclined shape when compared to the other shapes. It is noted here that resistance to flow and stresses on wall gives higher magnitude for converged shape, while the graphical illustration of velocity and temperature profile gives higher magnitude for divergent shape. Trapping is a motivating phenomenon for to show blood flow configuration in an inclined stenotic artery and here this configuration is discussed from Figs. (20) to (29). In Figs. (20) to (23), it is depicted that number of trapping bolus decreases with an increase in $G_r$ and $\beta$. The effects of nanoparticles volume fraction $\Phi$ are given in Figs. (24) and (25). It is noted here from this pattern that the trapping bolus decreases with an ncrease in nanoparticles volume fraction.

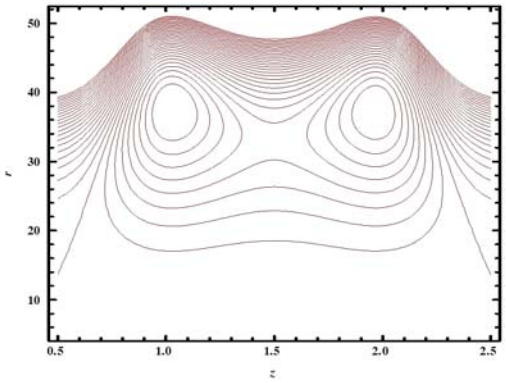


**Fig. 24. Blood flow configuration for $\Phi = 0.011$.**

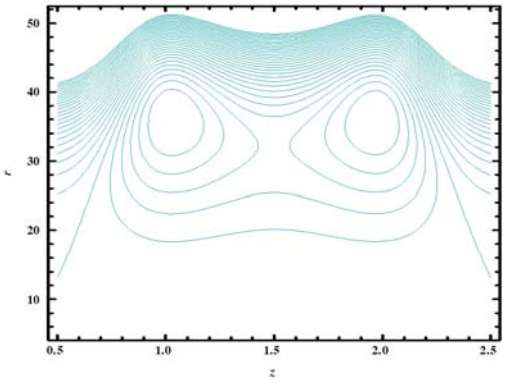


**Fig. 25. Blood flow configuration for $\Phi = 0.013$.**

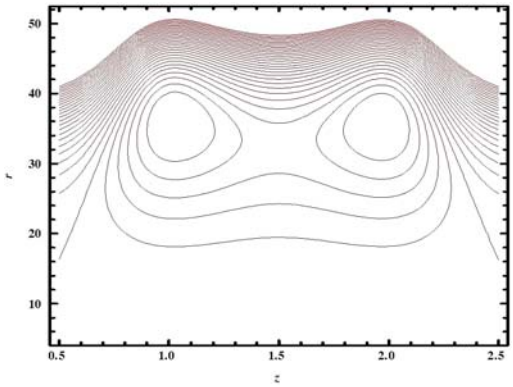


**Fig. 26. Blood flow configuration for $\delta = 0.08$.**

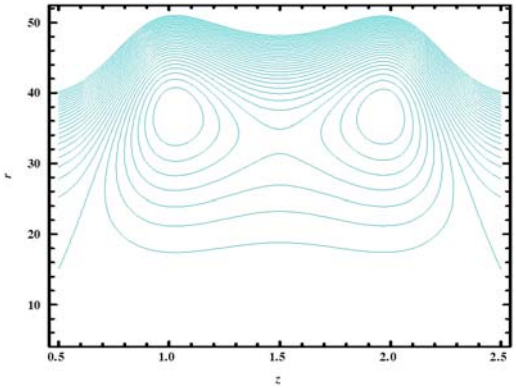


**Fig. 27. Blood flow configuration for $\delta = 0.09$ .**

.

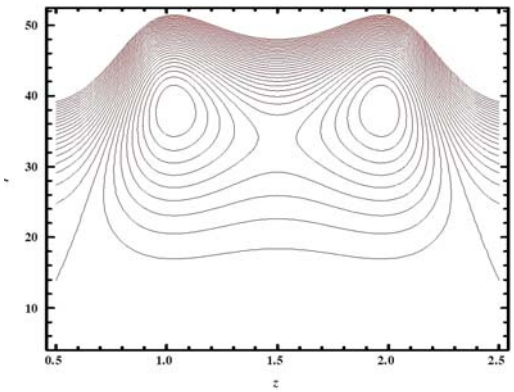


**Fig. 28. Blood flow configuration for $\delta_1 = 0.00$.**

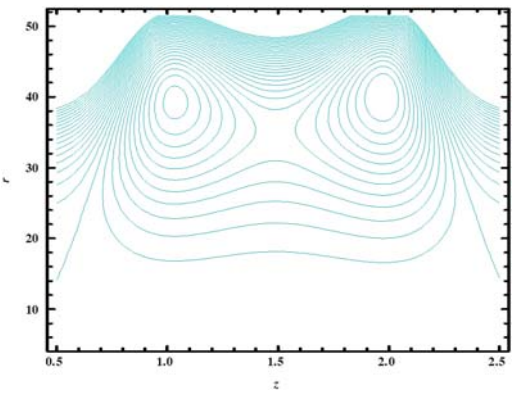


**Fig. 29. Blood flow configuration for $\delta_1 = 0.09$.**

The trapping configuration for stenosis height $\delta$ and maximum height of balloon $\delta_1$ are given in Figs. (26) to (29). It is depicted from this flow pattern that the number of trapping bolus increases with an increase in the values stenosis height, while trapping bolus increases in left side of inclined artery as compare to the right side of inclined artery with an increase in the values maximum height of the balloon. Table (2) is constructed to understand the numeric behavior of velocity profile for axial displacement of the balloon. One may observe from this table that the velocity profile for axial displacement $z_d$ increases throughout the inclined stenotic artery ( $H \le r \le h$ ). It is also analyzed that velocity profile gives higher magnitude for convergent shape of artery when compare to other shapes

## 4. CONCLUSION

The nanoparticle with balloon model through inclined stenotic artery is deliberated in this theoretical examination. The significant remarks from this study can be concise as follows

**Table 2 Variation of velocity profile for axial displacement of the balloon**

| Diverging shape | | | | Converging shape | | | Non-tapered shape | | |
|---|---|---|---|---|---|---|---|---|---|
| *r* | $z_d$=0.00 | $z_d$=0.05 | $z_d$=0.09 | $z_d$=0.00 | $z_d$=0.05 | $z_d$=0.09 | $z_d$=0.00 | $z_d$=0.05 | $z_d$=0.09 |
| *H* | 0.00000 | 0.00000 | 0.00000 | 0.00000 | 0.00000 | 0.00000 | 0.00000 | 0.00000 | 0.00000 |
| 0.2 | 0.10813 | 0.10840 | 0.10858 | 0.11091 | 0.11117 | 0.11135 | 0.10946 | 0.10972 | 0.10990 |
| 0.3 | 0.16063 | 0.16086 | 0.16102 | 0.16456 | 0.16479 | 0.16494 | 0.16250 | 0.16273 | 0.16289 |
| 0.4 | 0.18640 | 0.18658 | 0.18670 | 0.19071 | 0.19089 | 0.19101 | 0.18845 | 0.18863 | 0.18875 |
| 0.5 | 0.19512 | 0.19527 | 0.19537 | 0.19933 | 0.19947 | 0.19957 | 0.19713 | 0.19727 | 0.19737 |
| 0.6 | 0.19157 | 0.19170 | 0.19179 | 0.19532 | 0.19545 | 0.19553 | 0.19336 | 0.19349 | 0.19357 |
| 0.7 | 0.17873 | 0.17886 | 0.17894 | 0.18176 | 0.18189 | 0.18197 | 0.18018 | 0.18031 | 0.18039 |
| 0.8 | 0.15884 | 0.15898 | 0.15907 | 0.16093 | 0.16107 | 0.16116 | 0.15985 | 0.15998 | 0.16007 |
| 0.9 | 0.13379 | 0.13394 | 0.13404 | 0.13476 | 0.13492 | 0.13503 | 0.13426 | 0.13442 | 0.13453 |
| 1.0 | 0.10532 | 0.10549 | 0.10561 | 0.10502 | 0.10521 | 0.10534 | 0.10520 | 0.10538 | 0.10551 |
| 1.2 | 0.07514 | 0.07535 | 0.07549 | 0.07346 | 0.07368 | 0.07383 | 0.07437 | 0.07459 | 0.07473 |
| *h* | 0.00000 | 0.00000 | 0.00000 | 0.00000 | 0.00000 | 0.00000 | 0.00000 | 0.00000 | 0.00000 |

- Temperature phenomenon reduces for nanoparticle volume fraction, which shows that thermal conductivity of solid particles are helpful to dissipate heat.
- The hemodynamics of inclined stenotic artery give higher magnitude for the convergent shape when compare to other shapes.
- Stress on wall of stenotic inclined artery increases with an increase in inclination angle.
- Solid nanoparticle diminishes the hemodynamic effect that is experienced by blood while flowing in elastic stenosed inclined artery.
- Resistance to flow and stress on wall has same behavior versus $t$ and this wavering magnitude is higher for the convergent case.

## REFERENCES


Akbar, N. S. (2014). Metallic nanoparticles analysis for the peristaltic flow in an asymmetric channel with MHD. *IEEE Transactions on Nanotechnology* 13, 357-361.

Akbarzadeh, M., S. Rashidi, M. Bovand and R. Ellahi (2016). A sensitivity analysis on thermal and pumping power for the flow of nanofluid inside a wavy channel. *Journal of Molecular Liquids* 220, 1-13.

Buongiorno, J. (2005). Convective transport in nanofluids. *Journal of Heat Transfer* 128, 240-250.

Chakraborty, U. S., D. Biswas and M. Paul (2011). Suspension model blood flow through an inclined tube with an axially non-symmetrical stenosis. *Korea-Australia Rheology Journal* 23, 25-32.

Chakravarty, S. and P. K. Mandal (1996). A nonlinear two-dimensional model of blood flow in an overlapping arterial stenosis subjected to body acceleration. *Mathematical and Computer Modelling* 24, 43-58.

Choi, S. U. S. (1995). Enhancing thermal conductivity of fluids with nanoparticles, In: Siginer DA, Wang HP (eds), Developments and applications of non-Newtonian flows. *ASME* 36, 99-105.

Dash, R. K., G. K. Jayaraman and N. Mehta (1996). Estimation of increased flow resistance in a narrow catheterized artery: A theoretical model. *Journal of Biomechanics* 29, 917-930.

Ellahi, R., S. U. Rahman and S. Nadeem (2014). Blood flow of Jeffrey fluid in a catherized tapered artery with the suspension of nanoparticles. *Physics Letters A*, 378, 2973-2980.

Gentile, F., M. Ferrari and P. Decuzzi (2007). The Transport of Nanoparticles in Blood Vessels, The Effect of Vessel Permeability and Blood Rheology. *Annals of Biomedical Engineering* 36, 254-261.

Ijaz, S. and S. Nadeem (2016). Examination of nanoparticles as a drug carrier on blood flow through catheterized composite stenosed artery with permeable walls. *Computer Methods and Programs in Biomedicine 109*, 401-412.

Ijaz, S. and S. Nadeem (2016). Slip examination on the wall of tapered stenosed artery with emerging application of nanoparticles. *International Journal of Thermal Sciences 109*, 401-412.

Ismail, Z., I. Abdullah, N. Mustapha and N. Amin (2008). A power-law model of blood flow through a tapered overlapping stenosed artery. *Applied Mathematics and Computation* 95,669-

680.

Jiang, Y., C. Reynolds, C. Xiao, W. Feng, Z. Zhou, W. Rodriguez, S. C. J. Tyagi, W. Eaton, J. T. Saari and Y. J. Kang (2007). Dietary copper supplementation reverses hypertrophic cardiomyopathy induced by chronic pressure overload in mice. *The Journal of Experimental Medicine* 204, 657-666.

Liu, B. and D. Tang (2000). A numerical simulation of viscous flows in collapsible tubes with stenosis. *Applied Numerical Mathematics* 32, 87-101.

Mekheimer, Kh. S. and M. A. El Kot (2010). Suspension model for blood flow through arterial catheterization. *Chemical Engineering Communications* 197, 1195-1214.

Mekheimer, Kh. S. and Y. A. Elmaboud (2008). The influence of heat transfers and magnetic field on peristaltic transport of a Newtonian fluid in a vertical annulus: Application of an endoscope. *Physics Letters A*, 372, 1657-1665.

Mekheimer, Kh. S., F. A. Salama and M. A. El Kot (2015). The unsteady flow of a carreau fluid through inclined catheterized arteries have a balloon (angioplasty) with time-variant overlapping stenosis. *Walailak Journal of Science and Technology* 2015, 5-12.

Mekheimer, Kh. S., H. H. Mohammed and M. A. El Kot (2008). Induced magnetic field influences on blood flow through an anisotropically tapered elastic artery with overlapping stenosis in an annulus. *Canadian Journal of Physics* 89, 201-212.

Mekheimer, Kh. S., H. H. Mohammed and M. A. El Kot (2012). Influence of heat and chemical reactions on blood flow through an anisotropically tapered elastic artery with overlapping stenosis. *Applied Mathematics & Information Sciences* 2, 281-292.

Mohan, V., V. Prashad and N. K. Varshney (2013). Effect of inclination of an stenosed artery on Casson fluid flow with periodic body acceleration. *International Journal of Advanced Scientific and Technical Research* 4, 365-371.

Nadeem, S. and S. Ijaz (2015). Theoretical analysis of metallic nanoparticles on blood flow through tapered elastic artery with overlapping stenosis. *Transaction on Nanobiosciences.*

Nadeem, S. and S. Ijaz (2015). Theoretical analysis of metallic nanoparticles on blood flow through stenosed artery with permeable walls. *Physics Letters A* 379, 542-554.

Nadeem, S. and S. Ijaz (2016). Impulsion of nanoparticles as a drug carrier for the theoretical investigation of stenosed arteries with induced magnetic effects. *Journal of Magnetism and Magnetic Materials* 410, 230-241.

Nadeem, S. and S. Ijaz (2016). Theoretical examination of nanoparticles as a drug carrier with slip effects on the wall of stenosed arteries. *International journal of heat and mass transfer* 93, 1137-1149.

Prasad K. M. and G. Radhakrishnamacharya (2008). Flow of herschel-bulkley fluid through an inclined tube of non-uniform cross-section with a multiple stenosis. *Arch Mechanical* 60, 161-172.

Sankar, D. S. and K. Hemalatha (2007). Pulsatile flow of Herschel-Bulkley fluid through catheterized arteries: A mathematical model. *Applied Mathematical Modelling* 31, 1497-1517.

Srivastava, V. P. and R. Srivastava (2009). Particulate suspension blood flow through a narrow catheterized artery. *Computers and Mathematics with Applications* 58, 227-238.

Texon, M. (1957). A hemodynamic concept of atherosclerosis with particular reference to coronary occlusion. *Archives of Internal Medicine* 99, 418-430.

Vermaa, N., K. Mishra, S. S. U. Siddiqui and R. S. Gupta (2011). Study of blood flow through a catheterized artery. *Advances in Applied Science Research* 2 114-122.

Young, F. D. and F. Y. Tsai (1973) Flow characteristics in model of arterial stenosis steady flow. *Journal of Biomechanics* 6, 395-410.